Quantitative and detailed spatiotemporal patterns of drought in China during 2001–2013

Article *in* Science of The Total Environment · July 2017

DOI: 10.1016/j.scitotenv.2017.02.202

8 authors, including:

Lei Zhou
National Environmental Monitoring Center
19 PUBLICATIONS **141** CITATIONS
SEE PROFILE

Jianjun Wu
Beijing Normal University
58 PUBLICATIONS **644** CITATIONS
SEE PROFILE

Xinyu Mo
Chinese Academy of Sciences
9 PUBLICATIONS **57** CITATIONS
SEE PROFILE

Qianfeng Wang
Fuzhou University
21 PUBLICATIONS **126** CITATIONS
SEE PROFILE

Science of the Total Environment 589 (2017) 136–145

Contents lists available at ScienceDirect

Science of the Total Environment

journal homepage: www.elsevier.com/locate/scitotenv

Quantitative and detailed spatiotemporal patterns of drought in China during 2001–2013

Lei Zhou [a,b,*], Jianjun Wu [c], Xinyu Mo [d], Hongkui Zhou [c], Chunyuan Diao [e], Qianfeng Wang [f], Yuanhang Chen [b], Fengying Zhang [b]

[a] School of Surveying and Mapping Engineering, Beijing University of Civil Engineering and Architecture, Beijing 102616, China
[b] China National Environmental Monitoring Center, Beijing 100012, China
[c] Academy of Disaster Reduction and Emergency Management, MOCA/MOE, Beijing Normal University, Beijing 100875, China
[d] State Key Laboratory of Remote Sensing Science, Institute of Remote Sensing and Digital Earth, Chinese Academy of Science, Beijing 100101, China
[e] Department of Geography, University at Buffalo, The State University of New York, Buffalo, NY 14261, United States
[f] College of Environment and resource, Fuzhou University, Fuzhou 350116, China

HIGHLIGHTS

- A quantitative drought monitoring index ISDI was used to identify spatial patterns of drought over China.
- The spatial distribution of drought intensity has a strong correlation with eco-geographical regionalization in China.
- The regions with higher drought probabilities were most distributed in the south and north of China.
- This study shows valuable in informing the future drought prevention measures and management policies.

GRAPHICAL ABSTRACT

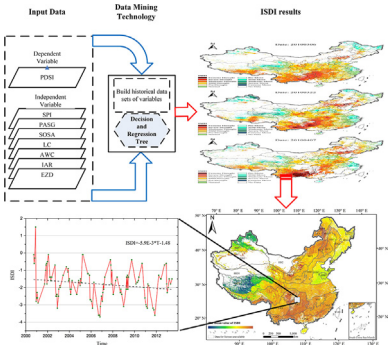

ARTICLE INFO

Article history:
Received 26 December 2016
Received in revised form 20 February 2017
Accepted 25 February 2017
Available online xxxx

Editor: Jay Gan

Keywords:
Drought
ISDI
China
Spatiotemporal patterns

ABSTRACT

Investigation of spatiotemporal patterns of drought is essential to understand the mechanism and influencing factors of drought occurrence and development. Due to the differences in designation of various drought indices, it remains a great challenge to obtain an accurate result in spatiotemporal patterns investigation of drought. In this study, a quantitative drought monitoring index (i.e., Integrated Surface Drought Index, ISDI) was used to identify spatiotemporal patterns of drought and the drought variation trend at the pixel level during 2001–2013 over China. Eco-geographical regionalization was used as an evaluation unit to distinguish the ecological and climatic background of drought over the whole country. The results showed that the spatial distribution of drought intensity has a strong correlation with eco-geographical regionalization in China. The severe drought areas were mainly concentrated in sub-humid regions and semi-arid regions of medium temperate zones, and humid regions of middle subtropical zones. The regions with higher drought probabilities were most distributed in the south and north of China, while the regions in central and western China exhibited lower drought probabilities. The most obvious decreasing trend of ISDI from 2001 to 2013 was located in the northeast of China and south of the Yangtze River. This decrease in ISDI over time indicates a trend for progressive aggravation of

* Corresponding author at: School of Surveying and Mapping Engineering, Beijing University of Civil Engineering and Architecture, Beijing 102616, China and China National Environmental Monitoring Center, Beijing 100012, China.
E-mail address: zhoulei8341@163.com (L. Zhou).

http://dx.doi.org/10.1016/j.scitotenv.2017.02.202

drought severity in these areas. This study shows great promise in informing the future drought prevention measures and management policies under the background of more frequent extreme climate events.

1. Introduction

Drought affects a large number of people and causes more losses to society compared to other natural disasters (Wilhite, 2000). China is one of the most densely populated agricultural countries in the world, and meanwhile is a drought disaster-prone country. The frequent occurrence of drought poses an increasingly severe threat to the Chinese agricultural production (Li et al., 1999). Under global warming, extreme climate events, especially droughts, have occurred more frequently in recent years over increasingly larger areas (Liang et al., 2014). Since 2009, the more frequent recurrence of extreme droughts has gravely affected the livelihood of farming communities in large geographical regions of China and has resulted in severe impacts on crop yields (Wang et al., 2014). Both southwestern and mideastern China have suffered from the most severe droughts during the past sixty years, which have caused enormous impacts on agriculture, food supplies, industries, the national economy, human health and ecosystems (Han et al., 2014).

Drought has complex spatial and temporal characteristics (Brown et al., 2008). Investigation of spatiotemporal patterns of drought provides a basis to understand the mechanism and influencing factors of drought occurrence and development. It is also beneficial to forecast future droughts and potential vulnerabilities (Mallya et al., 2016). Because drought may cause agricultural production reduction and then increases food insecurity, the understanding of drought characteristics and drought change trend help to minimize the drought impacts (Potop, 2011; Wang et al., 2014). On a global scale, the drought trend has been discovered mainly using meteorological data (Dai, 2011; Sheffield et al., 2012). There were also lots of studies focused on investigating the spatiotemporal patterns of drought in China using various drought indices (Huang et al., 2015; Liu et al., 2016; Wang et al., 2014; Xu et al., 2015b). Most of these studies were carried out on region, province, or climate zone scale, and often based on one certain drought index (Li et al., 2013). However, at the eco-geographical region level, spatiotemporal drought characteristics has high correlation with the comprehensive condition of climate, topography and land cover types (Wu et al., 2015). Drought pattern investigation at eco-geographical region level based on integrated drought index helps to get more accurate and comparable information which is very important for drought understanding.

Timely and accurate drought monitoring is an important means for spatiotemporal patterns investigation of drought (Mishra and Singh, 2010). In recent years, an increasing number of researchers have paid attention to accurate drought monitoring and management (Du et al., 2013; Tadesse et al., 2008). Due to the complex characteristics of drought, a variety of drought indices, including meteorological-based and satellite-based indices, have been developed for drought monitoring throughout the world (Mishra and Singh, 2011). These drought indices have their own advantages as well as weaknesses and shortcomings. On one hand, meteorological-based indices are based on site observations. The meteorological sites are only distributed in certain locations and not uniformly distributed over space, and thus the spatiotemporal patterns of drought revealed by meteorological-based indices may not be representative or accurate. On the other hand, satellite-based indices are usually developed according to the vegetation stress conditions or soil moisture. Although satellite-based drought indices can provide near real time drought condition detection over the globe at a relatively high spatial resolution, these indices are usually not only affected by drought, but may also be affected by a combination of other factors (e.g., flooding, fire, plant diseases and insect pests, hail damage). It is difficult to distinguish drought-related vegetation stress from that caused by other factors without additional information (Brown et al., 2008).

In recent years, several integrated drought indices (e.g., China Integrated Drought Monitor (CI), United States Drought Monitor, and Integrated Surface Drought Index (ISDI)) that comprehensively consider meteorological data and satellite data have been devised (Rhee et al., 2010; S. Pulwarty and Sivakumar, 2014). Most of these indices are integrated into regional or national operational online drought systems that release and update real-time drought monitoring results (Svoboda, 2000; Svoboda et al., 2002; Zhang et al., 2009). Among the indices, Integrated Surface Drought Index (ISDI) was particularly desirable. It takes into account various climate-based drought indices, satellite-based vegetation indices, Land Surface Temperature (LST), and biophysical and topographical conditions to produce 1-km regional drought condition maps at 16-day intervals (Wu et al., 2015). The validation of ISDI results confirmed that ISDI is capable of monitoring the near real time drought severity at a relatively high spatial resolution. It shows great promise in guiding the drought management and mitigation in China.

Most of drought patterns and tendency investigations employed meteorological drought indices such as PDSI or Standardized Precipitation Index (SPI) (Xu et al., 2015a; Yu et al., 2013). However, the conclusions of these studies were not completely consistent, for the methods used were different. Moreover, because of the spatial discretization and non-uniform distribution of meteorological sites, the detailed spatial patterns of drought investigation is still a challenge. There were also some studies based on satellite derived drought indices (Cunha et al., 2015; Li et al., 2013; Liang et al., 2014). Li et al. (2013) found that most parts of China were getting wetter in growing seasons by using satellite derived indices from 1982 to 2005. For the limitation of satellite-based drought indices in quantitative drought monitoring, the spatial patterns of drought intensity was difficult to be described by these indices (Wu et al., 2015). Due to a wide range of meteorological-based or satellite-based indices selected for drought monitoring, the research conclusions of the spatiotemporal distribution patterns and the change trend of drought in China from different studies were usually not consistent (Wang et al., 2014). Therefore, an integrated drought monitoring index that leverages the current meteorological-based and satellite-based indices to examine the spatial and temporal patterns of drought is urgently needed. ISDI provides a robust tool for spatiotemporal patterns investigation of drought in China.

Drought has close relationship with climate condition and ecological system. Vegetation growth, soil moisture are directly influenced by droughts (Cunha et al., 2015; Wang et al., 2015a). In tropical wetland ecosystems, drought also can be used for predicting forest fire danger (Taufik et al., 2015). Meteorological condition (e.g. precipitation, temperature) is the main driving factors of drought (Huang et al., 2015; Liu et al., 2016; Xu et al., 2015b). Meanwhile, drought has obvious impact on ecosystem (Assal et al., 2016; Wang et al., 2015b). Many studies have begun to study the characteristics and trend of drought in river basin or geographical regionalization scale (Li et al., 2013; Ndehedehe et al., 2016; Tadesse et al., 2015), and these methods are more accurate to reveal the characteristics and trends of drought information than in administrative division. The eco-geographical regionalization is more comprehensive than climatic regionalization and geographic zoning because it combines the integrated information of meteorology, topography, and land surface cover types. However, there were few studies focused on drought characteristics and trends variation in different eco-geographical regions. The existing researches were mainly about the impacts of droughts on the ecosystem (Kahil et al., 2015; Słowiński et al., 2016; Zhang et al., 2016).

In this study, the ISDI will be used to investigate: i) spatial patterns of drought at the 1 km × 1 km pixel scale and the variation characteristics in different eco-geographical regions; ii) The trend of drought over China in eco-geographical regionalization scale. The near-real-time detailed spatial patterns of drought over China detected by ISDI will be of great significance for understanding the mechanisms and influencing factors of drought at various spatial and temporal scales.

2. Data and methods

2.1. Study area

The mainland China including Hong Kong, and Macau was selected as our research area. The terrain of China is complex and diverse, with large mountainous area (accounted for about 2/3). The topography of China is low-lying west to east. China covers large area and the ecological climate characteristics in different regions are obviously different. There are 49 eco-geographical regions in mainland of China (Zheng, 2008). In different eco-geographical region, the air temperature, precipitation, topography, agro-type and crop planting system vary enormously. Precipitation is the main source of water in the large area, while temperature is the influence factor of evapotranspiration. The relationship between temperature and precipitation is the dominant factor of drought risk in a region. Therefore, the investigation of spatiotemporal patterns of drought is necessarily to be carried out in different eco-geographical regions over China.

2.2. ISDI time series dataset

2.2.1. Overview of ISDI model

Based on big data analysis method, ISDI is an integrated surface drought monitoring index which was developed to quantitatively detect the drought intensity at 1 km * 1 km spatial resolution and near real time results (Wu et al., 2013; Wu et al., 2015; Zhou et al., 2013). ISDI can reflect the comprehensive information of vegetation conditions, surface thermal and water content environment related to drought characteristics. Several biophysical variables were integrated to ISDI model for distinguishing the regional difference of drought characteristics. ISDI results had been successfully used for drought monitoring over China and proved its accuracy and detailed drought information detection capacity from 2001 to 2013 (Wu et al., 2015).

The ISDI time series dataset from 2001 to 2013 over China were produced at 16-day interval. There are 9 variables integrated to conduct ISDI results. Two meteorological drought indices named Palmer Drought Severity Index (PDSI) and SPI were used for quantifying drought detection at site scale. The spatial continuous variables derived from satellites were Vegetation Supply Water Index (VSWI) and Start of Season Anomaly (SOSA). The remote sensed variables were not only used for standardizing spatial estimation of drought severity, but also for reflecting vegetation conditions, surface thermal and water content environment caused by drought. The biophysical datasets were used for distinguishing drought characteristics differences. The selected biophysical datasets include digital elevation data (DEM), ecological zoning data (EZD), irrigated agriculture region data (IAR), land cover data (LC), and soil available water capacity (AWC). PDSI and SPI were site-scale and all the other variables were raster-scale. 9 × 9 km window was used to extract the historical sequence dataset of all variables at the corresponding time.

A big data analysis model named Classification and Regression Tree (CART) algorithm (Cubist 2.07) was used in our study to train historical datasets of all variables. The outputs of Cubist were a series of rule-based, linear regression formulas. The inputs of Cubist were divided into two parts, one dependent variable and many independent variables. Because PDSI is based on principle of water balance and can quantitatively monitor drought intensity, PDSI was chosen as dependent variable. All the other datasets were selected as independent variables. ISDI modeled for three different seasons (spring, summer, and autumn) respectively for ground vegetation has different sensitivities to water in three growing seasons (Zhou et al., 2013). We used 10-fold cross-validation method for each seasonal training dataset to evaluate the modeling accuracy. Finally, the generated three seasonal sub-models were used to calculate ISDI results pixel by pixel. There were 11, 23, and 20 regression rules derived for spring, summer, and autumn season respectively. One of the generated regression rules were as follows:

Rule: If: SOSA > 10, SPI ≤ 0.43, Elevation ≤ 1724, AWC ≤ 260, Eco_region in (semi-arid region)

Then: ISDI = −2.107 + 3.67 SPI − 0.0005 Elevation + 0.004 AWC

Among the independent variables, only SPI was original site-scale data and was interpolated to 1 × 1 km raster format based on Inverse Distance Weighting (IDW) method. The ISDI construction flowchart was follows.

The classification of generated ISDI is shown in Table 1.

2.2.2. The original database of ISDI

2.2.2.1. Remote sensing data and meteorological data. As mentioned above, the original datasets used in our study included three parts, named remote sensing data, meteorological data, and biophysical data. The remote sensing data include three Moderate Resolution Imaging Spectroradiometer (MODIS) products, the Normalized Difference Vegetation Index (NDVI) (MOD13A2, 16-day, 1 km × 1 km), Land Surface Temperature (LST) (MOD11A2, 8-day, 1 km × 1 km), and yearly Land Cover (LC) products (MCD12Q1, yearly, 1 km × 1 km). MODIS products were acquired from the MODIS data distribution center (http://ladsweb.nascom.nasa.gov/data/search.html). The meteorological data used in our study include daily average temperature, minimum temperature, maximum temperature, and precipitation. The gauge observed climate data were obtained from 752 standard surface meteorological sites over China. The daily meteorological data from 1961 to 2013 was derived from the China Meteorological Data Sharing Service System (http://cdc.cma.gov.cn/). In order to ensure the enough time series data of climate data used to calculate drought indices, 497 weather sites' data among 752 basic climate sites was extracted to generate PDSI and SPI sequence data. The sites with >1 day missed observation data were eliminated in the original datasets.

2.2.2.2. Drought indices generated from the original data. VSWI and SOSA were calculated based on MODIS products. VSWI is used for reflecting the land surface and vegetation drought condition by the result of NDVI and LST ratio. Before this, the average value of adjacent LST images were calculated to covert 8-day LST to 16-days. This method maintained the remote sensed drought indices all have 16-day temporal resolution. SOSA was calculated using smoothed NDVI time series data to account for the timings of stating season anomaly caused by drought (Brown et al., 2008; Wu et al., 2013). The Start of Season Time (SOST) was defined as the time when the change rate of NDVI curve reached the maximum value.

Two meteorological drought indices named PDSI and SPI were calculated based on daily climate data. SPI has been successfully used for quantitatively drought condition detection over the world. SPI offers advantages in comparable results in different regions and various time scale. Firstly, the Γ probability distribution function was used to simulate the precipitation distribution. Normal standard treatment was used to calculate the precipitation probability distribution. Finally, SPI was derived using the precipitation accumulation frequency. The 12-month and 9-month scale SPIs were used in our study to generate ISDI in our study (Brown et al., 2008; Wu et al., 2013). The precipitation probability density function was as follows:

$$f(x) = \frac{1}{\beta^{\gamma}\Gamma(x)} x^{\gamma-1} e^{-x/\beta}, x>0 \quad (1)$$

Table 1
Drought degree classification of ISDI.

Grades	Drought	ISDI
1	Normal	$-1 < ISDI \le 1$
2	Milds	$-2 < ISDI \le -1$
3	Moderate	$-3 < ISDI \le -2$
4	Severe	$-4 < ISDI \le -3$
5	Extreme	$ISDI \le -4$

where β and γ are the scale and shape parameters respectively, which can be calculated using likelihood estimation method.

PDSI was calculated based on the water balance principle. The water balance equation was used to describe the precipitation reached the requirement of climate adaptation.

$$\hat{P} = \widehat{ET} + \hat{R} + \widehat{RO} - \hat{L}, \tag{2}$$

Here $\hat{P}$is precipitation, $\widehat{ET}$ is evapotranspiration, $\hat{R}$ is supplementary water capacity, $\widehat{RO}$ is volume of runoff under suitable climate conditions, and $\hat{L}$ is water loss. By this equation, the water deficiency degree can be caught when the water supply is lower than the water supply compared to normal climatic conditions. Land surface temperature data was also integrated in PDSI to calculate potential evapotranspiration. PDSI was finally derived using the water deficiency degree compared with precipitation reached demand under suitable climate situations.

2.2.2.3. Biophysical data. There were several biophysical datasets used in our study to distinguish drought characteristics in various regions. The biophysical datasets were DEM, EAD, IAR, AWC, as well as the MODIS LC product. Earth environment conditions are different in various altitudes. Vegetation type, climatic situation, soil type, topographic features differences along with the change of altitude are all obvious influence factors of drought characteristics. EAD was selected to reflect the plant species and planting system differences in different regions. IAR data was used to describe the artificial mitigation effect on drought through irrigation. AWC was the variable to reflect the soil capacity to hold water available for plants. MODIS LC products were used for providing the information of land surface cover type. Although many of variables used in our study provided some parts of similar information of drought influence factors, the big data analysis tool Cubist has the ability to extract the valuable information of drought from training database. Cubist also has the advantages of distinguishing the amount of information contribution in regression process, and give different weights in generated rules (Wu et al., 2013; Wu et al., 2015).

DEM derived from Science Data Center of Cold and Arid Region in China (http://westdc.westgis.ac.cn/), with 1 km spatial resolution. EAD was extracted from China's Eco-geographical Regional Map (Zheng, 2008). IAR was acquired from distribution map of global irrigation area (GIAM10km-8classes:Version2.0) published by International Water Management Institute (IWMI). AWC was derived from Profile Available Water Capacity Map (10 km spatial resolution) published from International Geosphere-Biosphere Programme (IGBP). In order to maintain consistent spatial resolution, EAD, IAR, AWC and LC were resampled to 1 km spatial resolution using nearest neighbor assignment method in ArcGIS 10.2 software.

2.3. Temp-spatial analysis using ISDI

In order to investigate the spatial pattern of drought, the average value of ISDI at 16-days intervals during 2001–2013 was calculated at the 1 km × 1 km pixel scale. The average ISDI values in different eco-geographical regions were also calculated to evaluate the drought intensity differences at these regions.

Additionally, the spatial patterns of drought were investigated through calculating the frequency of drought occurrence ($ISDI < -1$) and the probability of various levels of drought intensity (i.e., mild, moderate, severe, and extreme) from 2001 to 2013 at the pixel scale. These spatial patterns were also examined in each eco-geographical region by aggregating the patterns of corresponding pixels.

To evaluate the trend of drought over time, linear regression model was used to fit the ISDI time series from 2001 to 2013 at the pixel level. The spatial pattern of the trend of drought was then analyzed at both the pixel level and the level of eco-geographical region. Chi-square test method was used to check the fitting goodness of the linear model. The equation of chi-square method was as follows:

$$\chi^2 = \sum_{i=1}^{r} \frac{(O_i - T_i)^2}{T_i} \tag{3}$$

where O_i is the number of observations of type i, r is the number of samples, and the T_i is the expected (theoretical) frequency of type r.

3. Results

3.1. The spatial pattern of drought

3.1.1. Spatial distribution of regional average ISDI

The spatial distribution of drought intensity (i.e., regional average ISDI) has strong correlation with eco-geographical regionalization (Fig. 2). The areas affected by drought (i.e., the areas of the reddish color in Fig. 2) were mostly distributed in the northern and southern parts of China. The severe drought areas were mainly concentrated in sub-humid regions and semi-arid regions of medium temperate zones, and humid regions of middle subtropical zones. Compared to the humid regions in middle subtropical zones, drought was more devastating in sub-humid regions of medium temperate zones (including middle Daxinganling Mountain steppe-forest region (IIB2), and hilly land of the north of western Daxinganling piedmont forest steppe region (IIB3)). In addition, the most serious drought area was found in eastern Inner Mongolia highland steppe region (IIC3) in semi-arid regions of medium temperate zones, with the average ISDI value close to −2. Similar severe drought areas also include some parts of northern and middle Loess Plateau steppe region (IIIC1) in semi-arid regions of warm temperate zone. (See Fig. 1.)

The average drought condition in most areas of humid region in middle subtropical zones was also very severe. Spatially, the serious drought affected area include Hunan and Guizhou mountainous evergreen broadleaved forest region (VA3), Sichuan basin evergreen broadleaved forest and cultivated vegetation region (VA4), and South of Eastern Himalayas mountain seasonal rainforest and evergreen broadleaved forest region (VA6). The average ISDI value in most of the above regions was between −1.5 and −2. There were also some other regions with average ISDI values between −0.5 and −1, such as southern Yangtze River hilly land evergreen forest and cultivated vegetation region (VA1), Fujian-Zhejiang and Nanling mountainous evergreen broadleaved forest region (VA2), and Yunnan Plateau evergreen broadleaved forest and pine forest region (VA5). In addition, the average drought condition in humid regions of southern subtropical zones was also unfavorable, including Fujian, Guangdong and Guangxi low mountainous and plain evergreen broadleaved forest and cultivated vegetation region (VIA2), and middle and southern Yunnan mountainous and hilly evergreen broadleaved forest and pine forest region (VIA3).

During 2001 to 2013, a slight humid condition was found in humid regions, sub-humid regions and arid regions of medium temperate zones, and semi-arid regions of plateau sub-cold zones. The medium temperate zones with a humid trend include Sanjiang plain wetland region (IIA1), Xiaoxinganling, and Changbai mountainous broadleaved and coniferous forest region (IIA2), and Piedmont platform of eastern

Song-Liao Plain broadleaved and coniferous mixed forest region (IIA3). The Plateau sub-cold zones with a humid trend include Southern Qinghai Plateau and wide valley alpine meadow-steppe region (HIC1), and Qiantang Plateau lake basin alpine steppe region (HIC2).

Among the typical humid regions, the most humid area was located in Qiangtang Plateau lake basin alpine steppe region (HIC2), with a regional average ISDI value of 1.34 during 2001–2013. The second most humid area was southern Qinghai Plateau and wide valley alpine meadow-steppe region (HIC1), with a regional average ISDI of 0.52 (Table 2). The total area of eco-geographical regions in dry conditions was more than that in humid conditions over China. Among the dry regions, the hilly land of the north of western Daxinganling piedmont forest steppe region (IIB3) was the driest area, with a regional ISDI value of −1.95 (Table 2). The following dry areas were southern east Himalayas mountainous seasonal rainforest and evergreen broadleaved forest region (VA6) and Hunan and Guizhou mountainous evergreen broadleaved forest region (VA3), with regional ISDI values of −1.69 and −1.63, respectively. The regional average values of ISDI in these dry regions all reached the mild drought level (Table 2).

3.1.2. Spatial distribution of drought frequency

According to the classification of ISDI, the frequency of drought occurrence and the probability of various drought intensity were calculated at the pixel scale (Fig. 3). From 2001 to 2013 at 16-day intervals, the high drought frequency regions were distributed in sub-humid regions and semi-arid regions of medium temperate zones, including middle Daxinganling mountainous steppe-forest region (IIB2), hilly land of the north of western Daxinganling piedmont forest steppe region (IIB3), southern Daxinganling steppe region (IIC2), and eastern Inner Mongolia highland steppe region. The drought frequently occurrence area also include northern and middle Loess Plateau steppe region (IIIC1), northern China mountainous deciduous broadleaved forest region (IIIB3), and Fenhe and Weihe River basins deciduous broadleaved forest, and cultivated vegetation region (IIIB4). Drought occurred >100 times in most of the aforementioned regions during the study period.

The average frequencies and probabilities of drought occurrence and intensity (i.e., mild, moderate, severe, and extreme) were calculated for each eco-geographical region (Table 3). There was a slight difference in the spatial distribution of drought probabilities and frequencies. The regions with higher drought probabilities were most distributed in the south and north of China, while the regions in central and western China exhibited lower drought probabilities. Most areas in humid regions of middle subtropical zones (located at south of the Yangtze River) had high probabilities of drought occurrence, with average drought probability over 60% and some area between 80% and 100%. In addition, the probability of total drought occurrence was also very high in Fujian, Guangdong and Guangxi low mountainous and plain evergreen broadleaved forest and cultivated vegetation region (VIA2) of southern subtropical zones, with a drought probability of >70% excluding missing data area.

As shown in Table 3, the region with highest drought frequency was hill land of north part of western Daxinganling piedmont forest steppe region (IIB3). Drought averagely occurred 123 times in this region. Drought occurred about 5.4 years during 13 years of study period, as the ISDI having 16-day scale. The probability of drought occurrence accounted for 80.6% of the valid data. Moreover, the drought intensity was more serious than other areas, with high occurrence frequency and probability of moderate, severe and extreme drought. Moderate, severe, and extreme drought occurrence frequency was 68, 20 and 7 times respectively, the corresponding occurrence probability of 44.4%, 13% and 4.6% respectively. IIB3 is most drought occurrence region among all eco-geographical zones.

Overall, drought frequency and probability were higher in humid, sub-humid, and semi-arid region in medium temperate zone than in semi-humid region, semi-arid region of warm temperate zone. The drought frequency and probability were lowest in middle subtropical zone and south subtropical zone. In high drought incidence area of medium temperate zone and warm temperate zone, the drought probability was between 53.9% and 80.6%, while that was between 60.5% and 72.1% in high drought incidence area of middle subtropical zone and south subtropical zone. On the whole, frequency and probability of moderate, severe and extreme drought were higher in medium

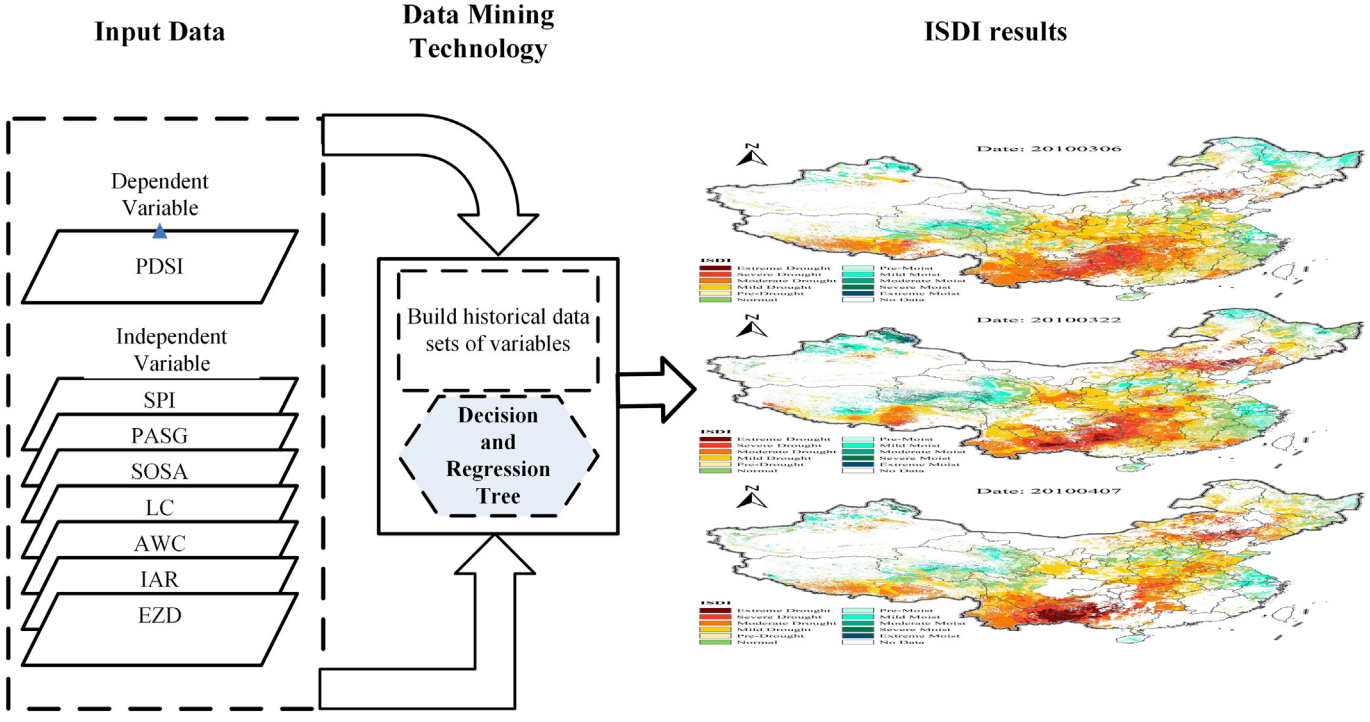

Fig. 1. Methodological flow-chart of ISDI.

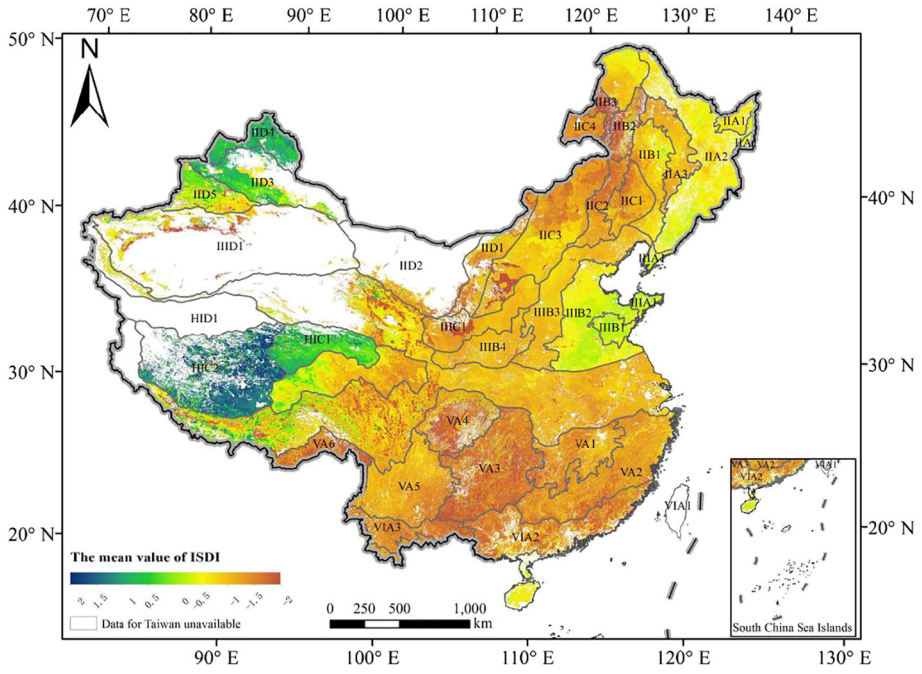

Fig. 2. The spatial distribution of mean values of ISDI during 2001 to 2013.

temperate zone and warm temperate zone than in middle subtropical zone and south subtropical zone. However, mild drought frequency and probability was high in middle subtropical zone and south subtropical zone. There was a high severe drought risk in medium temperate zone and warm temperate zone, while middle subtropical zone and south subtropical zone were more likely to encounter mild drought.

3.2. The trend of drought over China

Linear regression model was used to the fit ISDI series from 2001 to 2013 and chi-square test was used to test the significance of the fitting trend (Fig. 4). The linear model parameter a represents the increasing or decreasing degree of the fitted linear model. The chi-square test results were shown in Fig. 4(b). According to the critical value table of chi-square distribution, the trend of drought fitted in most parts of China was not significant (p value > 0.05). The areas that exhibited a statistically significant trend of drought (p value < 0.05) were mostly distributed in the south and southwest of China.

The areas that exhibited the most obvious decreasing trend of ISDI were distributed in the northeast of China and the south of the Yangtze River, and the decreasing trend in northeastern China was more pronounced than that in the south of the Yangtze River. The eco-geographical regions that showed obvious trends of drought in the northeast of China included middle Song-Liao plain forest-steppe region (IIB1), middle Daxinganling Mountain steppe-forest region (IIB2), and western Liaohe River plain steppe region (IIC1), with fitting decreasing trend values of −2 or lower. In addition, the eco-geographical regions that manifested obvious drought tendency in the south of the Yangtze River were mainly distributed in humid regions of middle subtropical zones, with fitting decreasing trend values of −1.5 or lower. These regions in the south of the Yangtze River included southern Yangtze River hilly land evergreen forest and cultivated vegetation region (VA1), Fujian-Zhejiang and Nanling mountainous evergreen broadleaved forest region (VA2), Hunan and Guizhou mountainous evergreen broadleaved forest region (VA3), and Sichuan basin evergreen broadleaved forest and cultivated vegetation region (VA4).

The time series of ISDI for a randomly selected pixel in Sichuan basin evergreen broadleaved forest and cultivated vegetation region (VA4) was shown in Fig. 5. The time series curve showed an obvious downward trend with typical fluctuation characteristics. The value of ISDI decreased about 0.6 during the study period according to the linear fitting result. The most severe drought occurred during the period 2006–2007. In addition, droughts in 2003, 2009, 2010, 2011, and 2012 were also very serious.

Table 2
The mean value of ISDI during 2001 and 2013 in the main eco-geographical regions.

Condition	Eco-geographical regions	Mean values of ISDI	STD
Humid	HIC1	0.52	0.46
	HIC2	1.34	0.76
	IIA1	−0.65	0.20
	IIA2	−0.53	0.20
	IIA3	−1.06	0.17
Dry	IIB2	−1.52	0.60
	IIB3	−1.95	0.31
	IIC3	−1.27	0.72
	IIIC1	−1.18	0.38
	VA1	−1.32	0.24
	VA2	−1.51	2.84
	VA3	−1.63	0.42
	VA4	−1.44	0.50
	VA5	−1.18	0.29
	VA6	−1.69	0.44
	VIA2	−1.45	0.41
	VIA3	−1.52	0.36

4. Conclusions

ISDI is a robust tool for investigating the spatial and temporal of drought in China. It integrated meteorological drought indices, vegetation condition indices, and the biophysical factors of drought. With the 1 km spatial resolution and near real time temporal resolution (16 days), ISDI offers a valuable solution to characterize the patterns of drought over space and time across China. The spatial patterns of drought and the drought variation trend were analyzed at the pixel scale during 2001–2013. The further investigation of spatiotemporal patterns of drought at the regional level can help understand the vulnerability of these eco-geographical regions to drought.

The results not only showed the regional patterns of drought, but revealed that the spatial distribution of drought intensity has strong

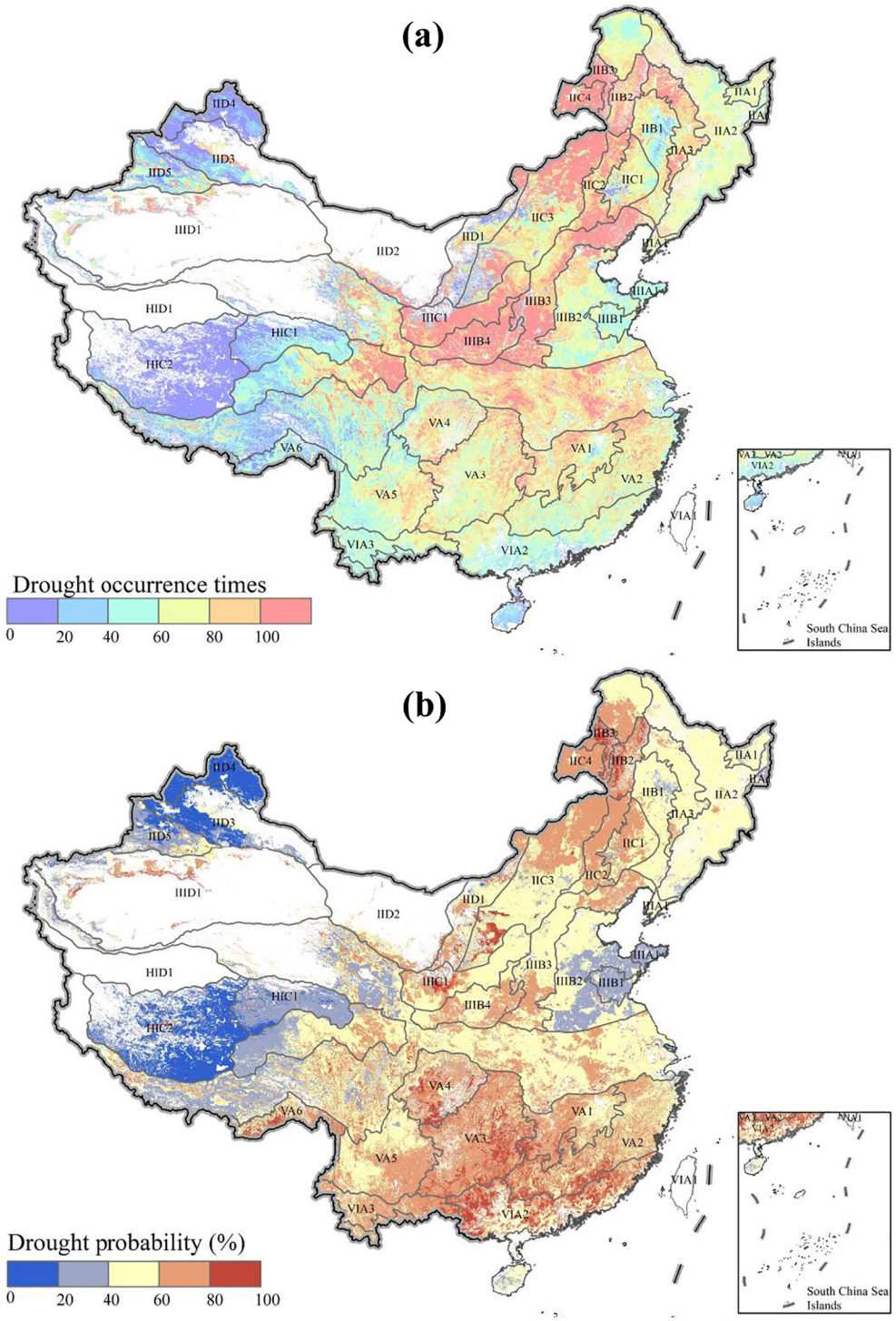

Fig. 3. The spatial distribution of drought occurrence times and drought occurrence probability during 2001 to 2013.

correlation with eco-geographical regionalization. It is beneficial to leverage eco-geographical regionalization as the evaluation unit to study the spatial and temporal patterns of drought in China. It is also beneficial to examine the drought differences among various eco-geographical zones.

The severe drought areas were mainly concentrated in sub-humid regions and semi-arid regions of middle temperate zones, and humid regions in middle subtropical zones. The areas affected by drought were mostly distributed in the northern and southern parts of China. During 2001 to 2013, a slight humid condition was found in humid regions, sub-humid regions, and arid regions of middle temperate zones, and semi-arid regions of plateau sub-cold zones. The eco-geographical regions that showed the highest drought frequency were distributed in sub-humid regions and semi-arid regions of middle temperate zones. The regions with higher drought probabilities were most distributed in the south and north of China, while the regions in central and western China exhibited lower drought probabilities.

The areas that exhibited the most obvious decreasing trend of ISDI were located in the northeast of China and the south of the Yangtze River, and the decreasing trend in northeastern China was more pronounced than that in the south of the Yangtze River. Thus, in terms of frequency, probability, and trend of drought, the areas in the northeast

Table 3
The average occurrence times and probabilities of drought and various drought condition during 2001 and 2013 in the main eco-geographical regions.

Regions	D_F	D_P	Mild_F	Mild_P	Moder_F	Moder_P	Sever_F	Sever_P	Extreme_F	Extreme_P
IIA3	92	53.9	30	18.0	51	30.0	9	5.3	1	0.7
IIB2	104	74.9	35	24.9	50	36.9	17	11.9	2	1.2
IIB3	123	80.6	29	18.6	68	44.4	20	13.0	7	4.6
IIC2	98	64.5	38	24.4	48	31.4	11	7.5	2	1.1
IIC3	86	58.1	36	23.7	35	23.3	12	8.1	4	3.0
IIIB3	101	56.2	69	38.6	24	13.6	6	3.6	1	0.4
IIIB4	105	59.4	74	41.9	23	13.1	7	4.2	0	0.2
IIIC1	97	57.8	44	26.0	39	22.7	14	8.5	1	0.6
VA1	82	66.0	51	41.6	24	19.2	6	4.9	0	0.3
VA2	73	65.1	48	42.3	17	15.4	7	6.0	1	1.4
VA3	78	71.4	30	27.2	38	34.4	9	8.4	1	1.4
VA4	76	67.8	41	36.5	24	22.0	9	8.1	1	1.2
VA5	66	60.5	48	43.8	13	12.1	4	3.3	1	1.3
VA6	40	67.9	13	21.1	22	36.3	5	10.0	0	0.5
VIA2	59	72.1	39	47.6	15	18.4	4	5.5	0	0.5
VIA3	61	67.0	24	26.7	30	33.4	5	5.4	1	1.5

D_F, Mild_F, Moder_F, Sever_F, and Extreme_F represent the average occurrence times (frequencies) of all levels of drought, mild drought, moderate drought, severe drought, and extreme drought, respectively. D_P, Mild_P, Moder_P, Sever_P, and Extreme_P represent the average probabilities of all levels of drought, mild drought, moderate drought, severe drought, and extreme drought, respectively.

of China and the south of the Yangtze River face the greatest challenge of aggravation of drought severity over time. Drought prevention measures and management policies should be strengthened in these areas to minimize the losses caused by drought in the future.

5. Discussion

This study was carried out to investigate the drought patterns and tendency over China based on the integrated drought index ISDI. Because of the complexity of the spatial and temporal characteristics of drought, the exact one drought index is not exist which can be used to fully describe drought information in various regions. Therefore, the existing drought characteristics results were not completely consistent because the drought indices used were different.

5.1. Drought patterns over China based on different drought indices

The reports of Intergovernmental Panel on Climate Change (IPCC) revealed that the globally warm days and nights will increase in the whole 21st century (Field et al., 2012). That means more drought events caused by increasing potential evapotranspiration will follow the higher temperature in the future (Sheffield et al., 2012). On a global scale, widespread drying area were found over Africa, East and South Asia, and other areas according to PDSI (Dai, 2011). In China, trend of PDSI decreased from 1950 to 2008 in Northeast and Southwest China (Dai, 2011). There were also results showed that the global drought area may be overestimated with the PDSI method although Northeast and Southwest China experienced more intense and longer droughts (Sheffield et al., 2012). Although there were some differences in the conclusions of the drought trend on global scale, the basically consistent existed on the results that drought become serious in many regions of China.

In China, two most severe drought events occurred in 1962–1963 and 2010–2011 according to SPI and Standardized Precipitation Evapotranspiration Index (SPEI) results (Xu et al., 2015b). North China Plain to downstream of Yangtze River, western part of North China Plain, Loess Plateau, Sichuan Basin, Yunnan-Guizhou Plateau had a significant drying trend caused by the decrease of precipitation (Xu et al., 2015b). Northeastern and Southwestern China were the typical regions showed obvious dry trend from 1982 to 2011 (Wang et al., 2015a). The spatial distribution of regional average ISDI also proved the previous study of drought patterns in China. However, the variation of droughts investigation in the ten basins of China showed that the whole country was generally getting wetter during 1982–2005 based on satellite-based Vegetation Condition Index (VCI) and Vegetation Health Index (VH) (Li et al., 2013). These differences are mainly caused by the differences between the meteorological drought indices and the satellite-based drought indices.

There were also a lot of studies focused on the regional drought patterns in China. In Yunnan province located in Southwestern China, the typical drying area, and large drought area were found in the whole region based on the composite index (CI) (Yu et al., 2013). Drought frequency analysis revealed the most severe drought period during 1960–2012 in Southwestern China (Xu et al., 2015a). In another typical drought area, Northeastern China, most parts of Inner Mongolia except for western and easternmost areas showed dry tendencies base on SPI and dry spells (DS) method (Huang et al., 2015). In summary, the drought distribution and trend changes of our study are consistent with the previous global, national and regional scale drought research results, although there are differences in detail. The main reason for the difference is the different drought indices used in the investigations. A case study showed that the drought characteristics obtained by satellite-based drought indices have obvious differences compared to that by meteorological drought indices (Wang et al., 2015b).

5.2. Drought indices selection effects on the results

Because of the different mechanism of drought indices, drought patterns and tendency results were not exactly consistent in the same region or during the same period. SPI is the most used drought index because it only based on precipitation data and comparable in various regions (Gunda et al., 2016). The limitation of SPI is lack of temperature data resulting in potential evapotranspiration deficiency in drought detection. Alternatively, PDSI is established based on water balance model and including temperature information to calculate evapotranspiration (Palmer, 1965). Compared to SPI, PDSI can reflect the drought intensity caused by the imbalance of surface water (Sheffield et al., 2012). Therefore, the drought patterns and tendencies derived by SPI and PDSI were not exactly the same (Wang et al., 2014; Xu et al., 2015b). However, SPI and PDSI are both based on the station measured meteorological data. The spatial representation of SPI and PDSI are restricted by the distribution of meteorological sites. Satellite-based drought indices are the good complement of site-based drought indices. VCI and VH were used to study drought variation in ten basins of china, but it showed great differences compared to the meteorological drought indices (Li et al., 2013). Satellite-based drought indices can get spatially continuous drought intensity distribution, but the accuracy of drought monitoring results need to be improved (Zhou et al., 2013). In recent years, the integrated drought indices which composed advantages of both meteorological drought indices and satellite-based drought indices were gradually

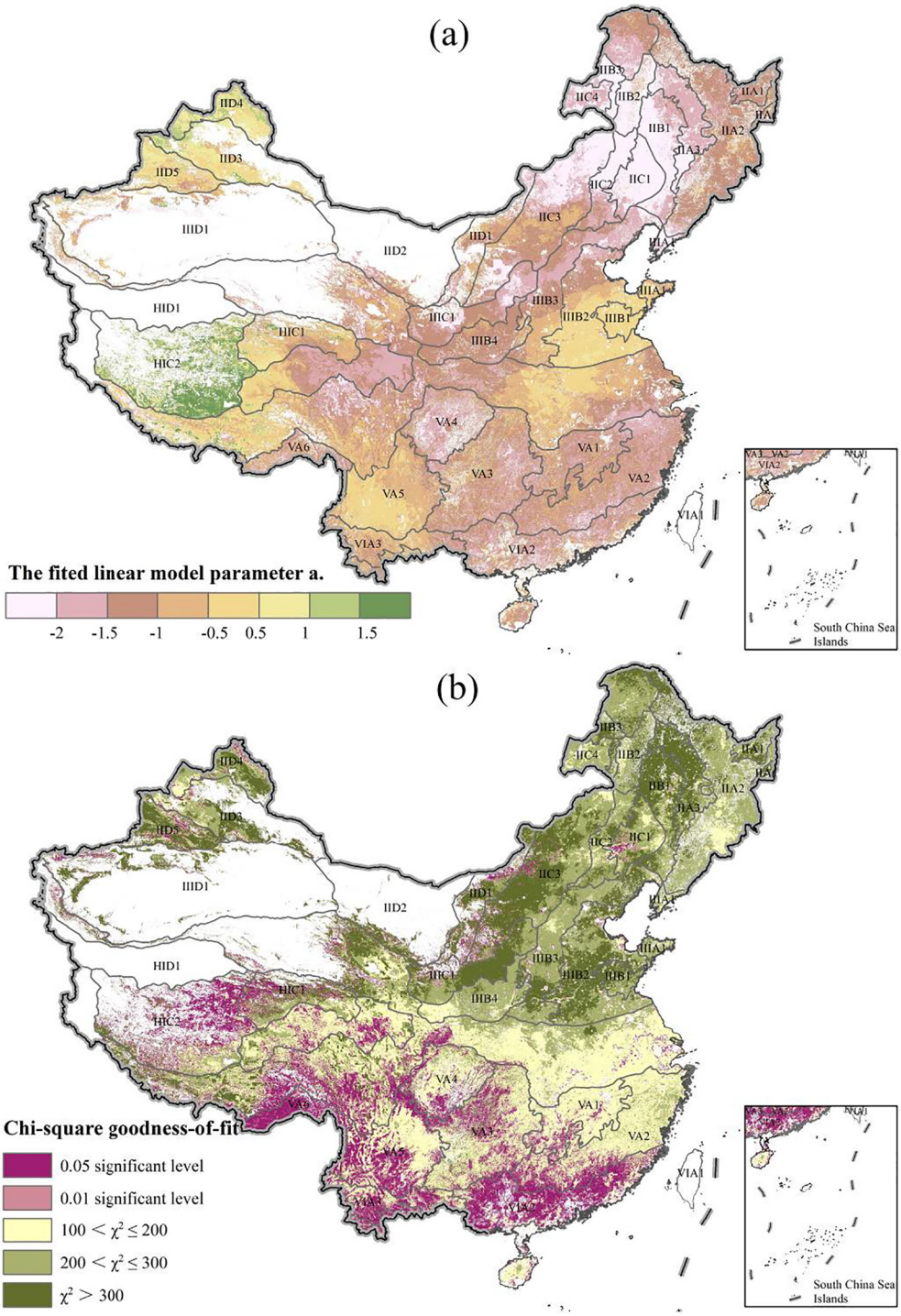

Fig. 4. The spatial distribution of the ISDI linear fitted model parameter *a* and the linear chi-square goodness-of-fit statistics.

used for drought study (Brown et al., 2008; Wu et al., 2015; Yu et al., 2013). Our investigation showed that ISDI is a robust tool for drought study because it integrated meteorological, remote sensing and drought influence factors data to get accurate and detailed drought condition.

Although ISDI has been successfully used for drought monitoring in China, there are still many works to do for its improvement. Further research is also needed to assess the possibility of other drought indices such as SPEI using as input variable of ISDI. Due to the limitation of MODIS time series data, the drought patterns was only investigated during 2001–2013 in our study. It is necessary to integrate other remote sensing data to extend the time series of ISDI. Frequent extreme drought events is a serious threat to food security. Therefore, national understanding of drought in China help to adjust drought management strategies for reducing agricultural drought losses.

Acknowledgements

This research received financial support from the Project 41501556 supported by National Natural Science Foundation of China. We are also grateful to Level 1 and Atmosphere Archive and Distribution System and China Meteorological Data Sharing Service System for providing remotely sensed and meteorological data in our research.

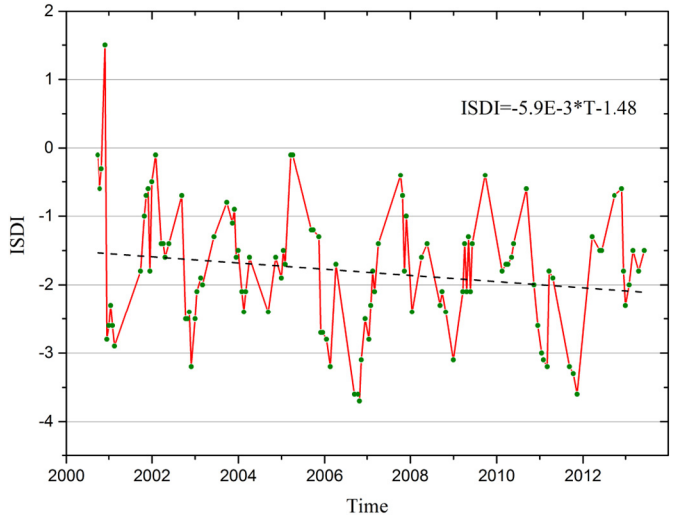

Fig. 5. Time series of ISDI at randomly selected sites in Sichuan Basin evergreen broadleaved forest and cultivated vegetation region (VA4) from 2001 to 2013.

Appendix A. Supplementary data

Supplementary data to this article can be found online at http://dx.doi.org/10.1016/j.scitotenv.2017.02.202.

References

Assal, T.J., Anderson, P.J., Sibold, J., 2016. Spatial and temporal trends of drought effects in a heterogeneous semi-arid forest ecosystem. For. Ecol. Manag. 365, 137–151.

Brown, J., Wardlow, B., Tadesse, T., Hayes, M., Reed, B., 2008. The Vegetation Drought Response Index (VegDRI): a new integrated approach for monitoring drought stress in vegetation. GISci. Remote Sens. 45, 16–46.

Cunha, A.P.M., Alvalá, R.C., Nobre, C.A., Carvalho, M.A., 2015. Monitoring vegetative drought dynamics in the Brazilian semiarid region. Agric. For. Meteorol. 214–215, 494–505.

Dai, A., 2011. Characteristics and trends in various forms of the Palmer Drought Severity Index during 1900–2008. J. Geophys. Res. Atmos. 116, D12115.

Du, L., Tian, Q., Yu, T., Meng, Q., Jancso, T., Udvardy, P., et al., 2013. A comprehensive drought monitoring method integrating MODIS and TRMM data. Int. J. Appl. Earth Obs. Geoinf. 23, 245–253.

Field, C.B., Barros, V., Stocker, T.F., Dahe, Q., 2012. Managing the Risks of Extreme Events and Disasters to Advance Climate Change Adaptation: Special Report of the Intergovernmental Panel on Climate Change. Cambridge University Press.

Gunda, T., Hornberger, G.M., Gilligan, J.M., 2016. Spatiotemporal patterns of agricultural drought in Sri Lanka: 1881–2010. Int. J. Climatol. 36, 563–575.

Han, L., Zhang, Q., Yao, Y., Li, Y., Jia, J., Wang, J., 2014. Characteristics and origins of drought disasters in Southwest China in nearly 60 years. Acta Geograph. Sin. 69, 632–639.

Huang, J., Xue, Y., Sun, S., Zhang, J., 2015. Spatial and temporal variability of drought during 1960–2012 in Inner Mongolia, north China. Quat. Int. 355, 134–144.

Kahil, M.T., Dinar, A., Albiac, J., 2015. Modeling water scarcity and droughts for policy adaptation to climate change in arid and semiarid regions. J. Hydrol. 522, 95–109.

Li, B., Su, H., Chen, F., Wu, J., Qi, J., 2013. The changing characteristics of drought in China from 1982 to 2005. Nat. Hazards 68, 723–743.

Li, K., Guo, Q., Zhang, J., 1999. China Drought Research and Disaster Mitigation Measures. Henan Science and Technology Press, Zhengzhou, China.

Liang, L., S-h, Zhao, Z-h, Qin, He, K.-x., Chen, C., Luo, Y.-x., et al., 2014. Drought change trend using MODIS TVDI and its relationship with climate factors in China from 2001 to 2010. J. Integr. Agric. 13, 1501–1508.

Liu, Z., Wang, Y., Shao, M., Jia, X., Li, X., 2016. Spatiotemporal analysis of multiscalar drought characteristics across the Loess Plateau of China. J. Hydrol. 534, 281–299.

Mallya, G., Mishra, V., Niyogi, D., Tripathi, S., Govindaraju, R.S., 2016. Trends and variability of droughts over the Indian monsoon region. Weather Clim. Ext. 12, 43–68.

Mishra, A.K., Singh, V.P., 2010. A review of drought concepts. J. Hydrol. 391, 202–216.

Mishra, A.K., Singh, V.P., 2011. Drought modeling — a review. J. Hydrol. 403, 157–175.

Ndehedehe, C.E., Awange, J.L., Corner, R.J., Kuhn, M., Okwuashi, O., 2016. On the potentials of multiple climate variables in assessing the spatio-temporal characteristics of hydrological droughts over the Volta Basin. Sci. Total Environ. 557–558, 819–837.

Palmer, W.C., 1965. Meteorological drought. U.S. Weather Bureau Research Paper 58.

Potop, V., 2011. Evolution of drought severity and its impact on corn in the Republic of Moldova. Theor. Appl. Climatol. 105, 469–483.

Rhee, J., Im, J., Carbone, G.J., 2010. Monitoring agricultural drought for arid and humid regions using multi-sensor remote sensing data. Remote Sens. Environ. 114, 2875–2887.

S. Pulwarty, R., Sivakumar, M.V.K., 2014. Information systems in a changing climate: early warnings and drought risk management. Weather Clim. Ext. 3, 14–21.

Sheffield, J., Wood, E.F., Roderick, M.L., 2012. Little change in global drought over the past 60 years. Nature 491, 435–438.

Słowiński, M., Marcisz, K., Płóciennik, M., Obremska, M., Pawłowski, D., Okupny, D., et al., 2016. Drought as a stress driver of ecological changes in peatland — a palaeoecological study of peatland development between 3500 BCE and 200 BCE in central Poland. Palaeogeogr. Palaeoclimatol. Palaeoecol. 461, 272–291.

Svoboda, M., 2000. An introduction to the drought monitor. Drought Netw. News 4, 15–20.

Svoboda, M., Lecomte, D., Hayes, M., Heim, R., Gleason, K., Angel, J., et al., 2002. The drought monitor. Bull. Am. Meteorol. Soc. 83, 1181–1190.

Tadesse, T., Haile, M., Senay, G., Wardlow, B.D., Knutson, C.L., 2008. The need for integration of drought monitoring tools for proactive food security management in sub-Saharan Africa. Nat. Res. Forum 32, 265–279.

Tadesse, T., Wardlow, B.D., Brown, J.F., Svoboda, M.D., Hayes, M.J., Fuchs, B., et al., 2015. Assessing the vegetation condition impacts of the 2011 drought across the U.S. Southern Great Plains using the Vegetation Drought Response Index (VegDRI). J. Appl. Meteorol. Climatol. 54, 153–169.

Taufik, M., Setiawan, B.I., van Lanen, H.A.J., 2015. Modification of a fire drought index for tropical wetland ecosystems by including water table depth. Agric. For. Meteorol. 203, 1–10.

Wang, H., Chen, A., Wang, Q., He, B., 2015a. Drought dynamics and impacts on vegetation in China from 1982 to 2011. Ecol. Eng. 75, 303–307.

Wang, H., Chen, Y., Pan, Y., Li, W., 2015b. Spatial and temporal variability of drought in the arid region of China and its relationships to teleconnection indices. J. Hydrol. 523, 283–296.

Wang, Q., Wu, J., Lei, T., He, B., Wu, Z., Liu, M., et al., 2014. Temporal-spatial characteristics of severe drought events and their impact on agriculture on a global scale. Quat. Int. 349, 10–21.

Wilhite, D.A., 2000. Drought as a natural hazard: concepts and definitions. In: Wilhite, D.A. (Ed.), Drought: A Global Assessment. Routledge, London & New York, pp. 3–8.

Wu, J., Zhou, L., Liu, M., Zhang, J., Leng, S., Diao, C., 2013. Establishing and assessing the Integrated Surface Drought Index (ISDI) for agricultural drought monitoring in mid-eastern China. Int. J. Appl. Earth Obs. Geoinf. 23, 397–410.

Wu, J., Zhou, L., Mo, X., Zhou, H., Zhang, J., Jia, R., 2015. Drought monitoring and analysis in China based on the Integrated Surface Drought Index (ISDI). Int. J. Appl. Earth Obs. Geoinf. 41, 23–33.

Xu, K., Yang, D., Xu, X., Lei, H., 2015a. Copula based drought frequency analysis considering the spatio-temporal variability in Southwest China. J. Hydrol. 527, 630–640.

Xu, K., Yang, D., Yang, H., Li, Z., Qin, Y., Shen, Y., 2015b. Spatio-temporal variation of drought in China during 1961–2012: a climatic perspective. J. Hydrol. 526, 253–264.

Yu, W., Shao, M., Ren, M., Zhou, H., Jiang, Z., Li, D., 2013. Analysis on spatial and temporal characteristics drought of Yunnan Province. Acta Ecol. Sin. 33, 317–324.

Zhang, J., Mu, Q., Huang, J., 2016. Assessing the remotely sensed Drought Severity Index for agricultural drought monitoring and impact analysis in North China. Ecol. Indic. 63, 296–309.

Zhang, Q., Pan, X., Ma, Z., 2009. Droughts. China Meteorological Press, Beijing.

Zheng, D., 2008. Study on Eco-geographical Regionalization System in China. Commercial Press, Beijing.

Zhou, L., Wu, J., Zhang, J., Leng, S., Liu, M., Zhao, L., et al., 2013. The Integrated Surface Drought Index (ISDI) as an indicator for agricultural drought monitoring: theory, validation, and application in mid-eastern China. IEEE J. Select. Topics Appl. Earth Observ. Remote Sens. 6, 1254–1262.